Am J Transl Res 2022;14(6):4350-4362
www.ajtr.org /ISSN:1943-8141/AJTR0142918

Original Article

Diffusion tensor imaging study of the microstructural changes in the white matter of patients with herpes zoster and postherpetic neuralgia

Jian Jiang[1*], Qing Huang[2*], Shuda Hong[1], Qing Luo[1], Xian Liu[1], Xiaoyan Hou[1], Lili Gu[3]

[1]Department of Radiology, The First Affiliated Hospital, Nanchang University, Nanchang 330006, Jiangxi, People's Republic of China; [2]Department of Radiology, Jiangxi Provincial Children's Hospital, Nanchang 330000, People's Republic of China; [3]Department of Pain, The First Affiliated Hospital, Nanchang University, Nanchang 330006, Jiangxi, People's Republic of China. [*]Equal contributors.

Received March 16, 2022; Accepted May 16, 2022; Epub June 15, 2022; Published June 30, 2022

Abstract: Objective: To determine the association between white matter structural changes and PHN by analyzing the diffusion tensor imaging data of patients with herpes zoster (HZ) or postherpetic neuralgia (PHN), and the volunteered healthy controls (HC). Methods: A total of 48 participants with HZ, 40 participants with PHN, and 28 age and sex matched HC were enrolled in this study. The diffusion tensor imaging data were collected by a Siemens 3.0T magnetic resonance scanner, and FSL (FMRIB's software) was used to analyze the differences in diffusion indexes among the HZ, PHN and HC groups. In addition, the correlation between the image and the clinical parameters was analyzed. Results: The results indicated that the microstructural integrity of the white matter, which affects the information exchange and integration between pain and non-pain related brain regions, showed difference in patients with HZ and PHN. Conclusion: The study may provide an experimental basis for more thorough longitudinal research in the future to explore the changes of brain structure in patients with PHN from HZ and develop adequate treatment strategy.

Keywords: Diffusion tensor imaging, herpes zoster, postherpetic neuralgia, dispersion property

Introduction

Herpes zoster (HZ) is an infection caused by varicella zoster virus (VZV). It mainly manifests as aggregated herpes, erythema, and neuropathic pain in the affected skin [1]. HZ is self-limited. With the improvement of herpes, the acute pain symptoms disappear. Postherpetic neuralgia (PHN) is one of the most common complications of HZ [2]. A standard definition of PHN has not been defined yet. The commonly accepted diagnostic criterion is the persistence of local pain for over a month after herpes subsides [3]. PHN is a common chronic neuropathic pain syndrome, characterized by persistent burning pain and itching. The pain is often sharp, and hyperalgesia and abnormal painful sensations are observed [4]. It can be accompanied by sleep disorders, mood changes, depression and anxiety, and cognitive function changes [5]. This kind of pain has a profound impact on the physical and mental health and quality of life of patients, and increases the economic burden of society [6]. The pathogenesis of PHN is complicated, including age, herpes, pain, and skin lesions. Age is a significantly important independent factor that is positively correlated with the incidence of PHN, especially in people aged between 50 and 79 years old [4]. This may be due to the decline in body immunity and resistance caused by aging. With the increase in age, the incidence of PHN increases significantly [7], which makes the search for effective treatment of PHN more urgent.

The pathogenesis of PHN is complex and has not been fully understood. Today, most scholars agree that there is a dual mechanism involving the peripheral and central nervous system. The peripheral mechanism mainly involves the reactivation of latent herpes zoster virus, which can

cause degeneration and edema of peripheral neurons and nerve fibers, inflammation, demyelination, necrosis and adhesion of fibers, resulting in ectopic discharge of damaged nerve fibers and mutual mixed transmission induced discharge of neurons [8]. Another study found that the pain associated with PHN was not positively correlated with the damage degree of peripheral nerve endings [9]. The abovementioned studies indicate that the occurrence and development of PHN are related to the damage of the peripheral and central nervous systems. However, current studies have little understanding on the central nervous mechanism of PHN. Some studies proposed that after the peripheral afferent sensory fibers are damaged, the activity of some fibers is enhanced [5]. The nerve fibers can equally cause excessive neural discharge by small non-painful mechanical stimulation. When a large number of abnormal nerve electrical impulses are introduced into the central nervous system, it may lead to the sensitization of the central nervous system, thus causing hyperalgesia and even plastic changes in the function and structure of the central nervous system [10].

Recently, with the rapid development of neuroimaging technology, a variety of magnetic resonance imaging (MRI) techniques are being widely used in the study of PHN and the central nervous mechanism of neuropathic pain. An MRI study has reported changes in brain structure and function in patients with PHN [11]. Patients with PHN have complex functional changes of the central nervous system and white matter dispersion abnormalities [12]. PHN patients had a wider range of gray matter lesions than HZ patients, involving both pain and non-pain related brain areas. However, the characteristics of white matter microstructural changes in patients with HZ and PHN are still unclear. Diffusion tensor imaging (DTI), a new method to visualize brain structure, is a special form of MRI. DTI is based on the direction of water molecules' movement and can reveal how brain tumors affect neuronal connectivity [13].

In order to further understand the relationship between white matter structural changes and PHN, three groups of participants including patients with HZ, PHN, and healthy controls (HC) were analyzed. DTI was used to observe abnormal diffusion in the white matter in patients with HZ, PHN, and in healthy controls. The correlation between the diffusion indexes and clinical parameters (visual analogue scale (VAS) score, course of disease) was compared among patients with HZ, PHN, and healthy controls.

Materials and methods

Volunteers

In this prospective study, 88 patients (including 48 patients with HZ, 40 patients with PHN, and 28 HC) were recruited and screened from the pain department of the First Affiliated Hospital of Nanchang University. All patients were diagnosed according to the criteria of the International Association for the study of pain (IASP) by two experienced pain physicians. Based on the IASP criteria, all confirmed patients underwent MRI scan within one day after inclusion in the study. All patients and HC met the requirements of MRI. All participants and their guardians signed informed consent forms as required. The VAS was used to evaluate the intensity of spontaneous pain (0-10 points, 0 point as no pain). The VAS score of all patients was more than 5 points, while that of HC was 0 point. According to the literature, we included 40 PHN patients (36-78 years old) with persistent pain for more than 30 days, and 48 HZ patients (46-75 years old) who had HZ within one month, which had not subsided [3]. All patients and HCs were required to be right-handed, and all patients were gender- and age-matched to HC. HC inclusion criteria: (1) participants with body mass index (BMI) within the normal range (19≤ BMI <24); (2) participants with no smoking or drinking; (3) participants without diseases in the heart, liver, kidney, digestive tract, respiratory tract, blood, and nerve system; (4) participants without mental illness, pain, or paresthesia; (5) participants with normal blood biochemical indices, blood routine, stool routine, urine routine, electrocardiogram, chest X-ray, abdominal B-ultrasound examinations; (6) participants without a history of drug abuse and family history of mental disorders. Exclusion criteria for HC: pregnant women, breast-feeding women, women who plan to become pregnant within 6 months, women in menstruation, volunteers in

other clinical trials or had donated blood within 3 months prior to the trial, volunteers with physical disabilities, volunteers with allergies, and volunteers taking other prophylactic or therapeutic medications.

Inclusion criteria for PHN and HZ: (1) patients who meet the diagnostic criteria of HZ and PHN; (2) patients developed HZ within one month before admission, and their condition was not alleviated; (3) PHN patients with pain lasting more than one month (>30 days) after herpes resolution; (4) patients with VAS >5. Exclusion criteria for PHN and HZ: (1) patients with herpes zoster in special parts (such as ear, eye or head and face); (2) patients with other acute or chronic pain conditions, such as headache, toothache, arthritis, lumbar or cervical diseases; (3) patients with a history of mental disorders, such as mood disorders, epilepsy or head injuries; (4) patients with any serious life-threatening diseases, such as severe pulmonary and cardiovascular diseases, malignant tumours, etc.; (5) patients with contraindications to MRI scanning, such as dentures or claustrophobia. This study was approved by the medical ethics committee of the First Affiliated Hospital, Nanchang University (Ethical number: (2020) Medical Research Ethics Review (1-45)).

3.0T SiemensTrioTIM superconducting MR scanner equipped with 8 channel cranial coils was used for the MRI inspection in this study. All the participants were scanned from head to foot in the supine position, with the head fixed using a foam cushion to reduce head movement. All the participants were permitted to wear earplugs to reduce the discomfort from the interference of the noise produced by the scanner. For scanning, the same standard head coil was used to transmit and receive MRI signals. Participants were told to close their eyes, keep their body relaxed, stay awake, and try not to think before the scan.

The scanning sequence data included (1) DTI diffusion weighting image acquired using single echo planar imaging sequence. Thirty diffusion sensitive gradient directions, B value = 1000, 2 repetitions; scanning without diffusion weighting (b = 0), 2 repetitions. Image acquisition parameters were as follows: repetition time (TR) = 6600 ms, echo time (TE) = 102 ms, matrix = 128 × 128; field of view (FOV) = 256 × 256 mm^3; excitation times (nex) = 2; slice thickness = 2 mm, interval = 0.2 mm, total 62 sections, and voxel size = 1 × 1 × 3 mm^3. (2) Conventional axial T2WI images: TR = 3000 ms, TE = 122 ms, matrix = 256 × 256, FOV = 240 mm × 240 mm, slice thickness = 5 mm, and total 19 sections; (3) conventional axial T1WI images: TR = 250 ms, TE = 2.46 ms, matrix = 256 × 256, FOV = 240 mm × 240 mm, slice thickness = 5 mm, and total 19 slices. We first performed conventional T1WI and T2WI transection scans to exclude organic lesions in the brain.

Data processing

FMRIB's software library (FSL, http://fsl.fmrib.ox.ac.uk/fsl/fslwiki/) was used for data analysis. During data processing, two radiologists initially carefully examined all DTI images to eliminate artifacts. Data processing was performed as follows: The Digital Imaging and Communications in Medicine format of DTI data were converted to NIfTI format by the dcm2niigui tool in FSL. The FMRIB's diffusion toolbox in FSL was used to perform head movement and eddy current corrections, and the brain extraction toolbox was used to peel off the scalp. At the same time, a brain mask with B = 0 was created. Finally, the whole brain template was applied to DWI images. The diffusion tensor of each voxel was calculated, and the scalar indexes of all participants were obtained, including fractional anisotropy (FA), mean dispersion coefficient (MD), radial dispersion coefficient (RD), and axial dispersion coefficient (AD).

Tract-Based Spatial Statistics (TBSS) analysis

TBSS analysis: (1) Image alignment: the FA of all participants were non-linearly registered to fmrib58 in the standard space of the Montreal Neurological Institute (MNI) 152 1 × 1 × 1 mm^3 FA standard template; (2) the average FA map and white matter skeleton were constructed based on all FA registered in standard space, and the average FA skeleton threshold was set as 0.2; (3) the average non-FA map and white matter skeleton were constructed based on the FA skeleton; and (4) the two sample unpaired t-test model in FSL was used to analyze the inter group diffusion indexes (FA, MD, RD and AD) by replacement nonparametric test. Age was used as the covariate, and the replacement parameter was 5000. The results of Threshold-Free Cluster

Table 1. Group characteristics

Clinical statistical data	PHN (n = 40)	HZ (n = 48)	HC (n = 28)	χ^2/Z/F value	*P* value
age	61.30±9.33[a]	58.04±10.46[a]	58.75±7.78[a]	2.486[c]	0.087
Sex (male/female)	13/27	22/26	9/19	2.173[d]	0.337
VAS score	6 (6, 7)[b]	6 (6, 7)[b]	-	0.506[e]	0.960
Course (day)	40 (30, 120)[b]	9 (5, 16.5)[b]	-	7.887[e]	<0.001

Note: HZ: herpes zoster; PHN: postherpetic neuralgia; HC: healthy control. a: According to the normal distribution measurement data, expressed with mean ± standard deviation; b: non normal distribution measurement data, expressed by median (interquartile interval). The following differences between groups were compared: c: age, ANOVA test; d: sex, chi-square test; and e: course and VAS score, nonparametric test.

Enhancement (TFCE) correction were considered statistically significant when the difference between groups was P<0.01. Results regions with more than 30 consecutive voxel sets with significant difference were regarded as the regions with significant results. The cluster output command was used to locate the coordinates and voxels of different brain regions. The atlas query tool was used to locate the white matter fibers in different brain regions. Johns Hopkins University (JHU) - icbm-dti-81 white matter labels atlas and JHU white matter tractography atlas were used to locate the white matter fiber bundles in different brain regions in the MNI space. For further correlation analysis, the regions with different TBSS results in HZ, PHN, and HC groups were taken as regions of interest, and the diffusion indexes (FA, MD, AD and RD) within these regions were extracted using FSL.

Statistical analysis

SPSS 24.0 software was used to describe and analyze the clinical data of all participants in the experiment. The ages of the HZ, PHN, and HC groups were analyzed by one-way ANOVA followed by Tukey's post-hoc test. The gender distribution comparison was conducted by a χ^2 test. A difference with a P<0.05 was considered statistically significant.

Results

Demographic statistics

No participant was excluded from the study. The final test samples included 40 PHN, 48 HZ, and 28 HC. The ages of the three groups were analyzed by a one-way ANOVA and multiple comparison test. The homogeneity test of variance yielded a f = 2, P = 0.368; the differences were not statistically significant (PHN vs HC, HZ vs HC, and PHN vs HZ, P = 0.338, 0.754, 0.148, respectively); there was no significant difference in gender distribution among the three groups based on the χ^2 test (PHN vs HC, HZ vs HC, and PHN vs HZ were P = 0.975, 0.241 and 0.203, respectively). The clinical characteristics of patients in the PHN, HZ, and HC group are shown in **Table 1**.

TBSS analysis results

Compared with those of the HC group, FA in some brain regions of the HZ group decreased significantly, while MD, AD, and RD increased significantly (P<0.01, TFCE correction). FA decreased significantly in the corpus callosum (knee, body, and splenium), bilateral corona radiata, bilateral anterior and posterior thalamus radiation, bilateral internal and external capsule, bilateral superior fronto occipital tract, bilateral superior and inferior longitudinal tract, bilateral fornix/stria terminalis, bilateral anterior cingulate gyrus, left uncinate tract, right cerebral peduncle, and bilateral corticospinal tract. The brain regions with significantly increased MD included the corpus callosum (knee, body, and splenium), bilateral corona radiata, bilateral thalamus anteroposterior radiation, bilateral internal and external capsule, right superior fronto occipital tract, bilateral lower fronto occipital tract, bilateral upper and lower longitudinal tract, left fornix/stria terminalis, bilateral uncinate tract, left cerebral peduncle, and bilateral corticospinal tract. The brain areas with significant elevation of AD included the splenium callosum, bilateral corona radiata, left anterior thalamic radiation, left internal capsule, bilateral external capsule, left upper and lower fronto occipital tract, left lower longitudinal tract, bilateral superior longitudinal tract, bilateral superior longitudinal tract, bilateral superior longitudinal tract, bilateral superior inferior frontal occipital tract, and left inferior longitudinal tract. The brain areas with

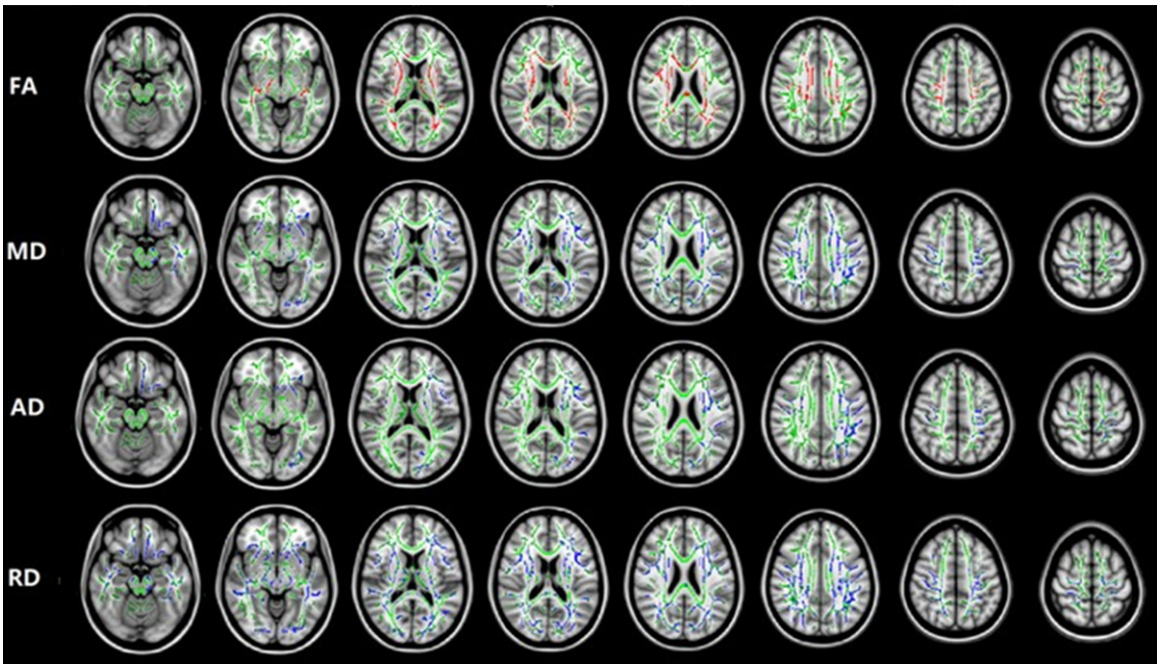

Figure 1. TBSS analysis results of white matter diffusion index in HZ group and HC group (P<0.01, TFCE correction). Green indicates the FA skeleton of all subjects, red indicates a decrease of indexes in patients with HZ, and blue indicates an increase.

Table 2. TBSS analysis of the difference in FA value between HZ group and healthy control group

Cluster	White matter fiber tracts	L/R/B	MNI coordinate (x, y, z)	Voxel Quantity
1	Knee of corpus callosum	-	(57, 109, 62)	20645
	The corpus callosum	-		
	Splenium of corpus callosum	-		
	Internal capsule	B		
	corona radiata	B		
	Postthalamic radiation	B		
	Prethalamic radiation	B		
	Lower longitudinal tract	B		
	Lower fronto occipital tract	B		
	Cerebral peduncle	R		
	Corticospinal tract	B		
	External capsule	B		
	Anterior cingulate gyrus	B		
	Fornix/stria terminalis	B		
	Upper longitudinal tract	B		
2	Prethalamic radiation	L	(93, 109, 66)	652
	Internal capsule	L		

Note: all tests had a P<0.01 and were corrected by TFCE multiple comparison. L: left. R: right. B: bilateral. x, y, z are the spatial coordinates of MNI152 template, z is the axial position of MNI152 template, and the unit of voxel value is mm^3.

significant increase in RD included the corpus callosum (body, pressure part), bilateral corona radiata, bilateral anterior thalamic radiation, bilateral internal and external capsule, bilateral upper and lower fronto occipital tract, bilateral upper and lower longitudinal tract, bilateral fornix/stria terminalis, bilateral uncinate tract, bilateral cerebral peduncle, and bilateral corticospinal tract (**Figure 1**; **Tables 2** and **3**).

Compared with those in the HC group, FA value was significantly decreased in some brain regions of the PHN group, while MD, AD, and RD values were significantly increased (P<0.01, TFCE correction). The brain regions with significant decrease in FA value included the corpus callosum (knee, body, and splenium), bilateral corona radiata, bilateral anterior and posterior thalamic radiations, bilateral internal and external capsules, bilateral inferior fronto occipital tract, bilateral upper and lower longitudinal tract, bilateral for-

Table 3. The comparison between the HZ and HC group with respect to MD, AD, and RD values in brain regions

Brain region	MD	AD	RD
Knee of corpus callosum	-		
The corpus callosum	-		-
Splenium of corpus callosum	-	-	-
Internal capsule	B	L	B
corona radiata	B	B	B
Postthalamic radiation	B		
Prethalamic radiation	B	L	B
External capsule	B	B	B
Lower longitudinal tract	B	L	B
Lower fronto occipital tract	B	L	B
Corticospinal tract	B	L	B
uncinate fasciculus	B	L	B
Fornix/stria terminalis	L		B
Upper longitudinal tract	B	B	B
Upper fronto occipital tract	R	L	B
cerebral peduncle	L		B

Note: all tests were P<0.01 and were corrected by TFCE multiple comparison, L: left. R: right. B: bilateral.

nix/stria terminalis, bilateral anterior cingulate gyrus, bilateral uncinate tract, bilateral cerebral peduncle, and bilateral corticospinal tract. The brain regions with significant increase in MD, AD and RD value included the corpus callosum (knee, body, and splenium), bilateral corona radiata, bilateral anterior and posterior thalamus radiation, bilateral internal and external capsules, bilateral inferior fronto occipital tract, bilateral superior and inferior longitudinal tracts, bilateral fornix/stria terminalis, bilateral anterior cingulate gyrus, bilateral uncinate tract, bilateral cerebral peduncle, middle cerebellar peduncle, bilateral posterior cingulate gyrus, and bilateral corticospinal tracts are increased (**Figure 2**; **Tables 4** and **5**).

Compared with those in the HZ group, MD, AD and RD values were significantly increased (P<0.01, TFCE correction) in some brain regions of the PHN group. The brain areas with significant increase in MD value included the corpus callosum (body, pressure part), right corona radiata, bilateral anterior and posterior thalamus radiation, bilateral internal and external capsule, bilateral inferior fronto occipital tract, bilateral superior and inferior longitudinal fasciculi, right lateral fornix/stria terminalis, bilateral anterior cingulate gyrus, bilateral uncinate tract, bilateral cerebral peduncle, bilateral frontal occipital tract, bilateral superior and inferior longitudinal fasciculus, right fornix/stria, bilateral anterior cingulate, middle peduncle of the cerebellum, left posterior cingulate gyrus, and bilateral corticospinal tracts. The brain regions with significant elevation of AD values included the corpus callosum (body and pressure part), right corona radiata, right thalamus anteroposterior radiation, right internal and external capsules, right inferior frontal occipital tract, right upper and lower longitudinal tracts, right fornix/stria terminalis, right anterior cingulate gyrus, right uncinate tract, right cerebral peduncle, and right posterior cingulate gyrus. The brain regions with significant increase in RD value included the corpus callosum (body, pressure part), corona radiata, bilateral anterior and posterior radiations of the thalamus, bilateral internal and external capsules, bilateral inferior fronto occipital tract, bilateral upper and lower longitudinal tracts, bilateral fornix/stria terminalis, left anterior cingulate gyrus, bilateral uncinate tract, bilateral cerebral peduncle, bilateral posterior cingulate gyrus, and bilateral corticospinal tract (**Figure 3**; **Table 6**). There was no significant difference in FA between the PHN and HZ groups.

Correlation analysis

When comparing PHN group with HZ group, the mean of the difference regions of MD, AD and RD values were positively correlated with their VAS scores, respectively. When HZ was compared to HC, the AD value of HZ got the similar results. The mean FA value in the region of considerably reduced FA was positively correlated with the disease duration of PHN when PHN was comparing with HC. Correlation analysis results of FA, MD, AD and RD values with VAS score and disease duration (days) in regions with differences are listed **Table 7**.

Discussion

DTI is a non-invasive imaging method based on the diffusion of water molecules in human brain. The difference in the direction and rate of free dispersion is detected and converted into images and parameters to obtain the structural integrity and spatial distribution of white matter fibers, such as uncinate and longitudinal bundles [10]. DTI has four parameter values: FA, MD, AD, and RD. FA is defined as the

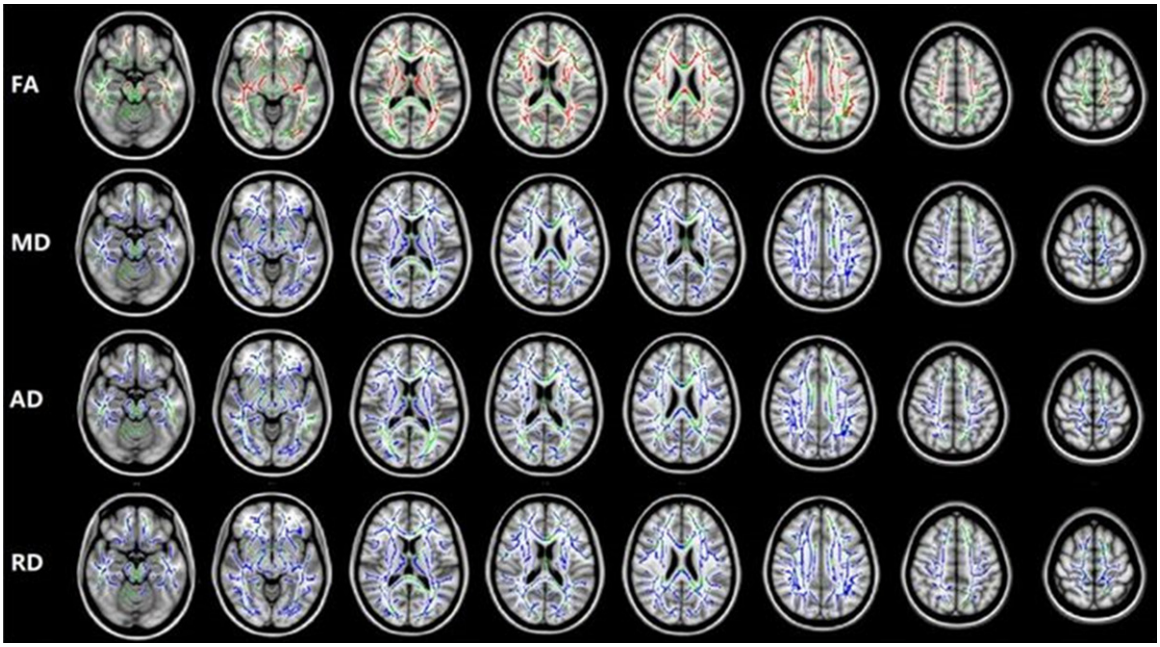

Figure 2. The results of TBSS analysis (P<0.01, TFCE correction) of white matter diffusion indexes in the PHN and HC groups (P<0.01, TFCE correction) showed that all subjects had an FA skeleton. Red indicates that the PHN group index decreased, and blue shows an increase.

Table 4. TBSS analysis of difference in FA value between the PHN and HC groups

cluster	White matter fiber tracts	L/R/B	MNI coordinate (x, y, z)	Voxel Quantity
1	Knee of corpus callosum	-	(102, 150, 90)	44062
	The corpus callosum	-		
	Splenium of corpus callosum	-		
	Internal capsule	B		
	corona radiata	B		
	Postthalamic radiation	B		
	Prethalamic radiation	B		
	Lower longitudinal tract	B		
	Lower fronto occipital tract	B		
	Cerebral peduncle	B		
	uncinate fasciculus	B		
	External capsule	B		
	Anterior cingulate gyrus	B		
	Fornix/stria terminalis	B		
	Upper longitudinal tract	B		

Note: all tests had P<0.01 and were corrected by TFCE multiple comparison. L: left. R: right. B: bilateral. x, y, z are the spatial coordinates of MNI152 template, z is the axial position of MNI152 template, and the unit of voxel value is mm^3.

proportion of the anisotropic component of water molecules in the whole diffusion tensor, reflecting the integrity of the myelin sheath of white matter fibers and the compactness and parallelism of the fibers [14]. MD value reflects the average dispersion ability of water molecules in all directions of tissues; AD and RD are the diffusion rates of water molecules in parallel and vertical axonal directions, respectively, in which AD value reflects the changes of axons [15] and RD value reflects the changes in the cell membrane and myelin sheath [16]. TBSS optimizes the alignment and smoothing of images based on non-linear registrations. This method is applicable to study the whole brain without pre-specifying the region of interest and can identify white matter abnormalities more accurately. Moreover, since the DTI indicators of individual subjects can be accessed, a more stable and reliable result will be yielded in the follow-up statistics [17, 18]. In recent years, as an imaging technique for quantitative analysis of the structural characteristics of white matter fibers, DTI has been widely

Table 5. Comparison of the PHN and HC groups with respect to MD, AD, and RD values in brain regions

Brain Region	MD	AD	RD
Knee of corpus callosum	-	-	-
The corpus callosum	-	-	-
Splenium of corpus callosum	-	-	-
Internal capsule	B	B	B
Corona radiata	B	B	B
Postthalamic radiation	B	B	B
Prethalamic radiation	B	B	B
External capsule	B	B	B
Lower longitudinal tract	B	B	B
Lower fronto occipital tract	B	B	B
Corticospinal tract	B	B	B
Uncinate fasciculus	B	B	B
Anterior cingutate	B	B	B
Fornix/stria terminalis	B	B	B
Upper longitudinal tract	B	B	B
Medipeduncle	-	-	-
Cerebral peduncle	B	B	B
Posterior cingutate	B	B	B

Note: all tests had P<0.01 and were corrected by TFCE multiple comparison, L: left. R: right. B: bilateral.

used in the study of various central encephalopathies, such as schizophrenia, cluster headache, Alzheimer's disease [17], and multiple sclerosis [5, 14, 19].

TBSS is an unbiased, voxel-by-voxel analysis of DTI data. Voxel based analysis (VBA) and TBSS are the most common methods for MRI-DTI data analysis. VBA has two significant shortcomings: uneven FA image registration boundary and no definite principle and standard for the arbitrary selection of a smoothing kernel [20]. TBSS overcomes these two shortcomings: alignment and smoothing issue. The nonlinear registration method and projection of the average FA skeleton solves the registration error. In addition, the analysis process of the TBSS method does not involve smoothing, so the need for selection of a smoothing kernel is avoided. Moreover, the dispersion characteristics of the white matter were analyzed systematically [21]. TBSS can initially measure the diffusion characteristics of water molecules, which can not only evaluate the brain microstructure, but also investigate the degree of myelination and fiber integrity. Beaulieu et al. reported that FA plays an important role in measuring the structural properties of the axon membrane, and the changes in FA values can also reflect the properties of myelin sheath [22]. In addition, the morphology and density of axons can also be reflected by FA and AD values [23]. Song et al. found in their study on mice that RD changes were closely related to the characteristics of myelination in the corpus callosum of mice, which could reflect the characteristics of changes in the structural integrity of myelin sheath with time progression [24]. The method of TBSS can be used to find differences in the microstructure of white matter in each group of subjects, and further explore the changes in the information of transmission process between different brain regions, thus providing a new technology and new ideas for revealing the brain structure and exploring central nervous system abnormalities.

In this study, the TBSS method was used to compare the differences in DTI diffusion indexes among HZ, PHN, and HC groups. The results showed that compared with that of HC, the diffusion properties of white matter fibers in patients with HZ and PHN were abnormal, indicating that the microstructural integrity of the white matter in patients with HZ and PHN was changed. Many studies have reported changes in the structure and function of the cortex and subcortical regions in patients with HZ and PHN [25, 26]; changes in brain regions including primary somatosensory cortex, thalamus, striatum, internal capsule, anterior cingulate gyrus, amygdala, hippocampus, posterior cingulate cortex, caudate nucleus, cerebellum, and fronto occipital temporal cortex, which are directly or indirectly related to pain, have been observed [26, 27]. Our results showed that compared with that in HC, the FA values of the corpus callosum and corona radiata, anterior and posterior radiation of the thalamus, internal and external capsules, superior and inferior fronto occipital tracts, superior and inferior longitudinal tracts, fornix/terminal stria, cingulate gyrus, uncinate tract, peduncle of cerebrum, and corticospinal tract were significantly decreased in patients with HZ and PHN, while MD, AD and RD values were increased, indicating that the integrity of the microstructure in these areas was destroyed; the white matter fiber connections in these regions involve information transmission and integration of pain sensation, memory, emotional motivation, and movement and affect the abnormal regulation

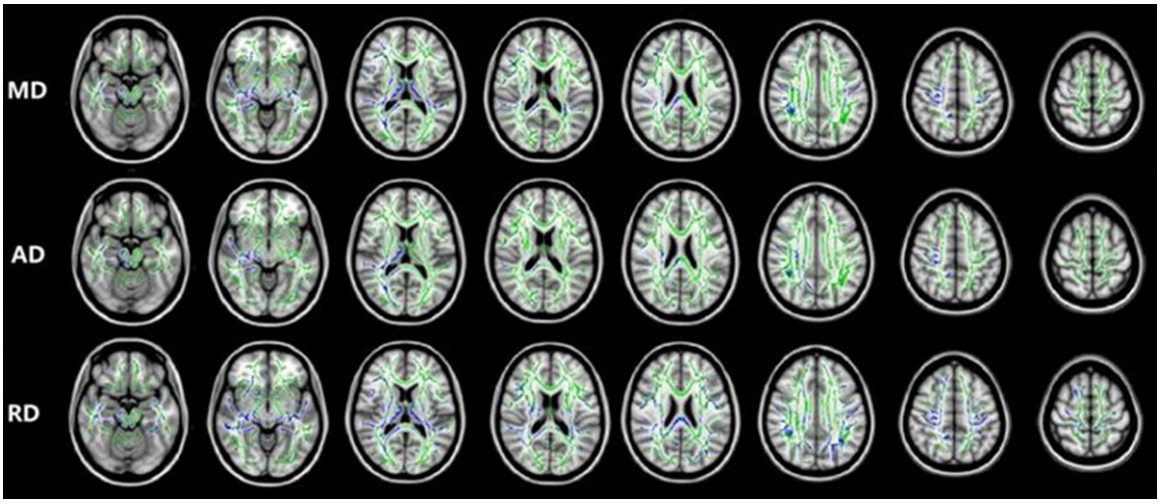

Figure 3. The results of TBSS analysis (P<0.01, TFCE correction) of the white matter diffusion index in the PHN and HZ groups (P<0.01, TFCE correction) showed that all subjects had an FA skeleton. Red shows that the PHN group had a decreased index, and blue shows an increased index.

Table 6. Comparison of PHN group and HZ group with respect to MD, AD, and RD values in brain regions

Brain Region	MD	AD	RD
The corpus callosum	-	-	-
Splenium of corpus callosum	-	-	-
Internal capsule	B	R	B
Corona radiata	R	R	B
Postthalamic radiation	B	R	B
Prethalamic radiation	B	R	B
External capsule	B	R	B
Lower longitudinal tract	B	R	B
Lower fronto occipital tract	B	R	B
Corticospinal tract	B	R	B
anterior cingulate cortex	B	R	L
Fornix/stria terminalis	R	R	B
Upper longitudinal tract	B	R	B
Uncinate fasciculus	B	R	B
Cerebral peduncle	B	R	B
Medipeduncle	-		
posterior cingulate cortex	L	R	B

Note: all tests had P<0.01 and were corrected by TFCE multiple comparison, L: left. R: right. B: bilateral.

of pain and cognitive and emotional disorders. The integrity of white matter fibers in patients with HZ and PHN changes, which affects the information exchange and integration of relevant brain regions and thus causes changes in the health status of patients. A previous study reported that the FA and AD values of pain-related and non-pain-related brain areas in patients with PHN were decreased, but there was no statistical difference in the MD and RD values [12]. It is speculated that the microstructural integrity change of white matter in patients with PHN is due to axonal degeneration without obvious demyelination, which is consistent with some results of the present study [15]. While a combined DTI and resting state functional MRI study in PHN patients showed that FA, MD, ALFF and/or fALFF indicated significant alterations in specific pain or pain-related brain regions [13], indicating disruption in both brain microstructure and function in patients with PHN.

MD, RD, and AD values of white matter fibers in some regions of patients with PHN were significantly increased when comparing with HZ, which indicated that there were differences in the integrity of white matter microstructure between patients with HZ and PHN. These different areas with white matter microstructural damage involve the inner and outer brain regions of pain. The corpus callosum is a white matter commissural fiber bundle that connects the two hemispheres and transmits information between the cerebral hemispheres. The corpus callosum-corona radiata-fronto-parietal-occipitotemporal cortex pathway is responsible for the integration of multi-dimensional sensory information, including cognitive control, attention, and emotional response [28]. Our previous research showed that the thick-

Table 7. Correlation analysis between diffusion index of different brain regions and clinical parameters ($^{R}/_{P}$)

Clinical Parameter	HZ vs HC				PHN vs HC				HZ vs PHN		
	FA	MD	AD	RD	FA	MD	AD	RD	MD	AD	RD
VAS score	0.495/	0.599/	0.839/	0.542/	0.349/	0.088/	0.101/	0.086/	0.715/	0.848/	0.681/
	0.102	-0.079	-0.030	-0.091	-0.152	0.283	0.263	0.275	0.040	0.021	0.045
Course (day)	0.127/	0.234/	0.216/	0.228/	0.997/	0.343/	0.290/	0.355/	0.001/	0.001/	0.002/
	0.223	0.175	0.182	0.117	0.001	0.154	0.171	0.150	0.344	0.390	0.333

ness of the bilateral primary visual cortex and right primary visual cortex, left somatosensory cortex, right anterior cingulate gyrus and medial prefrontal cortex increased in PHN patients [29], which is similar to the results of this study to some extent, indicating the corpus callosum-corona radiata-fronto-parietal-occipitotemporal cortex pathway was damaged in PHN patients. PCC is the core node at the back of the default network, and damage to the default network is the basis of cognitive and behavioral disorders [10]. The fornix originates from the hippocampus and projects to the papillary body, thalamus, and cingulate cortex of the hypothalamus through the internal capsule and connects the contralateral hippocampus through the fornix junction. The terminal stria is an important fiber connecting the amygdala and limbic system; the uncinate tract connects the prefrontal lobe, anterior cingulate gyrus, and limbic system. The fornix/stria terminalis, uncinate tract, anterior cingulate gyrus, thalamus, limbic system, and cerebral cortex constitute multiple pathways and participate in emotion regulation, energy balance, and reward processing [25, 27]. It is well known that a large number of white matter fibers connect the cortex and subcortical areas through the corticospinal tract, cerebral peduncle, middle cerebellar peduncle, longitudinal tract, frontal occipital tract, and internal and external capsule, and participate in the transmission and integration of information. In this study, we found that compared with the local white matter fiber dispersion of patients with HZ, that of patients with PHN was abnormal, which indicated that the integrity of white matter microstructure was changed, causing a communication disorder between the relevant brain regions and affecting the high-level central recoding definition of PHN. The results of the correlation analysis showed that the MD, AD, and RD values in the brain regions were positively correlated with the course of disease, our previous cortical thickness study also found that medial prefrontal cortex, frontal opercular cortex and left motor cortex were correlated with duration in PHN [29], indicating that the demyelination of the white matter, nerve fiber inflammation, and axonal lesions became increasingly more severe with the progression of PHN. However, no correlation was found between the diffusion indexes and pain intensity. In conclusion, compared with that of the HZ group, the changes of white matter microstructural integrity in patients with PHN are more extensive, and these brain regions may participate in the progression from HZ to PHN.

Based on the comprehensive analysis of the white matter diffusion indexes, the results showed that compared with that of the HC, the abnormal diffusion of white matter fibers in the HZ and PHN groups was characterized by decreased FA and increased MD, AD, and RD values. AD and RD values are considered imaging indicators reflecting the potential pathological changes of white matter [30]. The change of FA value was caused by changes in RD or RD and AD values [31]. There was no relationship between MD and FA in mathematical logic. MD value was positively correlated with demyelination, axonal edema and axonal decrease. Therefore, we believe that the damage in white matter microstructural integrity in patients with HZ and PHN is characterized by demyelination, nerve fiber inflammation, and axonal degeneration.

In the present study, MD and RD values in some brain regions of patients with PHN were significantly increased compared with those in the HZ group, and AD values were mainly in the right side of the brain and relatively limited. However, there was no significant difference in FA value between the PHN and HZ groups. FA changes are related to demyelination, axon loss and degeneration, and neuroinflammation.

There was no significant difference between the FA value of patients with PHN and HZ, which may be attributed to the nonhomogeneous changes of brain function and structure.

We noticed that the areas with changes in the diffusion indexes were not completely consistent between patients with HZ and PHN, which may be due to the different degrees of damage to the white matter microstructure in different regions. Conversely, it may be due to the different pathological information, which is reflected by different diffusion indexes.

Comparing previous DTI studies of PHN, we found that the alterations for FA and MD were more similar, and our study made a supplement to the changes in RD and AD. In conjunction with previous studies on chronic pain, increased AD, RD and MD may reflect abnormalities in neural axons and reduced neuronal density in the white matter of the brain in patients with HZ or PHN [32]. In our results, it indicated that PHN, HZ had increased AD, RD and MD compared to HC, and the changes in PHN were the most significant, these changes were positively correlated with VAS scores, suggesting that the pain is worsened with the raise in structural damage degree to nerve fibers. On the other hand, reduced FA and increased MD values may suggest direct tissue damage and reduced cell density in patients with PHN. Some previous studies have reported that swelling of glial cells may underlie changes in FA [33], and reduced FA can be induced by factors such as demyelination, lower cell density or different membrane permeability, and is regulated by features such as axon diameter and changes in fibrous organization, which may indirectly explain the changes in MD. In the correlation analysis, we found a positive correlation between FA values and disease duration in patients with PHN, which suggested that as the duration of pain increases, glial cells outside the nerve fibers may regenerate to compensate for the previously occurred damage, which was not found in previous experiments of PHN. In the other case, increased RD may be a biological marker of demyelination, but the exact mechanism is unknown and may be related to oedema, inflammation, and some studies have found that as the disease changes from acute to chronic, the information provided by changes in AD may be limited [34, 35]. This implies that the progression of HZ to PHN probably associated with further aggravation of demyelination, and that changes in MD and FA may be more important for the mechanism of this transformation.

Notably, some of the DTI metrics changes observed so far were similar to other types of chronic pain findings, such as trigeminal neuralgia, fibromyalgia, which further supported our hypothesis that brain white matter fiber changes potentially mediate the perception and regulation of chronic pain [36].

This study achieved preliminary results, but there are some limitations to this study, which will be improved upon in future studied. First, the sample of this study was relatively limited, and the courses of PHN was relatively short due to the time limitation, which cannot fully explain the small differences in white matter microstructural changes between acute and sequelae stages of HZ. In the future, we will recruit more patients with PHN with longer course. Second, none of the participants had obvious clinical symptoms of anxiety and depression, and we did not conduct professional cognitive and emotional assessments of the participants. However, some studies have shown that patients with PHN have depression and anxiety, which may affect the microstructure of white matter fibers [5]. In future studies, we will include cognitive and emotional assessments such as depression and anxiety. Finally, it is not clear whether the microstructural change of white matter was the primary cause of PHN pain or the secondary that caused by functional changes, and whether these structural changes would be ameliorated after relief from the disease. This is a limitation in all functional MRI studies on brain structure changes in patients with PHN. However, a more thorough longitudinal study in the future may help to explore the changes of brain structure in patients with PHN from HZ and to develop adequate treatment.

In summary, TBSS and DTI methods were used to reveal the changes of white matter microstructural integrity in patients with HZ and PHN; these changes affect the information exchange and integration between pain and non-pain-related brain regions. The changes of brain white matter microstructural integrity in patients with PHN are more extensive.

Acknowledgements

We are very grateful for the support of the Regional Science Foundation of National Natural Science Foundation of China (81960313) and General Project of the Natural Science Foundation of Jiangxi Provincial Science and Technology Department (20192BAB205039).

Disclosure of conflict of interest

None.

Address correspondence to: Lili Gu, Department of Pain, The First Affiliated Hospital, Nanchang University, Nanchang 330006, Jiangxi, People's Republic of China. Tel: +0791-88692748; E-mail: gll2009cn@aliyun.com

References

[1] Jeon YH. Herpes zoster and postherpetic neuralgia: practical consideration for prevention and treatment. Korean J Pain 2015; 28: 177-184.

[2] Johnson RW and Rice AS. Clinical practice. Postherpetic neuralgia. N Engl J Med 2014; 371: 1526-1533.

[3] Forbes HJ, Bhaskaran K, Thomas SL, Smeeth L, Clayton T, Mansfield K, Minassian C and Langan SM. Quantification of risk factors for postherpetic neuralgia in herpes zoster patients: a cohort study. Neurology 2016; 87: 94-102.

[4] Mounsey AL, Matthew LG and Slawson DC. Herpes zoster and postherpetic neuralgia: prevention and management. Am Fam Physician 2005; 72: 1075-1080.

[5] Chen L, Zhou R, Sun F, Weng Y, Ye L and Yang P. Efficacy and safety of the extracorporeal shockwave therapy in patients with postherpetic neuralgia: study protocol of a randomized controlled trial. Trials 2020; 21: 630.

[6] Friesen KJ, Falk J, Alessi-Severini S, Chateau D and Bugden S. Price of pain: population-based cohort burden of disease analysis of medication cost of herpes zoster and postherpetic neuralgia. J Pain Res 2016; 9: 543-550.

[7] Makharita MY, Amr YM and El-Bayoumy Y. Effect of early stellate ganglion blockade for facial pain from acute herpes zoster and incidence of postherpetic neuralgia. Pain Physician 2012; 15: 467-474.

[8] Dworkin RH, Gnann JW Jr, Oaklander AL, Raja SN, Schmader KE and Whitley RJ. Diagnosis and assessment of pain associated with herpes zoster and postherpetic neuralgia. J Pain 2008; 9 Suppl 1: S37-44.

[9] Opstelten W, McElhaney J, Weinberger B, Oaklander AL and Johnson RW. The impact of varicella zoster virus: chronic pain. J Clin Virol 2010; 48 Suppl 1: S8-13.

[10] Javad F, Warren JD, Micallef C, Thornton JS, Golay X, Yousry T and Mancini L. Auditory tracts identified with combined fMRI and diffusion tractography. Neuroimage 2014; 84: 562-574.

[11] Liu J, Hao Y, Du M, Wang X, Zhang J, Manor B, Jiang X, Fang W and Wang D. Quantitative cerebral blood flow mapping and functional connectivity of postherpetic neuralgia pain: a perfusion fMRI study. Pain 2013; 154: 110-118.

[12] Chen F, Chen F, Shang Z, Shui Y, Wu G, Liu C, Lin Z, Lin Y, Yu L, Kang D, Tao W and Li Y. White matter microstructure degenerates in patients with postherpetic neuralgia. Neurosci Lett 2017; 656: 152-157.

[13] Dai H, Jiang C, Wu G, Huang R, Jin X, Zhang Z, Wang L and Li Y. A combined DTI and resting state functional MRI study in patients with postherpetic neuralgia. Jpn J Radiol 2020; 38: 440-450.

[14] Teepker M, Menzler K, Belke M, Heverhagen JT, Voelker M, Mylius V, Oertel WH, Rosenow F and Knake S. Diffusion tensor imaging in episodic cluster headache. Headache 2012; 52: 274-282.

[15] Hong S, Gu L, Zhou F, Liu J, Huang M, Jiang J, He L, Gong H and Zeng X. Altered functional connectivity density in patients with herpes zoster and postherpetic neuralgia. J Pain Res 2018; 11: 881-888.

[16] Liu J, Gu L, Huang Q, Hong S, Zeng X, Zhang D, Zhou F and Jiang J. Altered gray matter volume in patients with herpes zoster and postherpetic neuralgia. J Pain Res 2019; 12: 605-616.

[17] Smith SM, Jenkinson M, Johansen-Berg H, Rueckert D, Nichols TE, Mackay CE, Watkins KE, Ciccarelli O, Cader MZ, Matthews PM and Behrens TE. Tract-based spatial statistics: voxelwise analysis of multi-subject diffusion data. Neuroimage 2006; 31: 1487-1505.

[18] Porter EJ, Counsell SJ, Edwards AD, Allsop J and Azzopardi D. Tract-based spatial statistics of magnetic resonance images to assess disease and treatment effects in perinatal asphyxial encephalopathy. Pediatr Res 2010; 68: 205-209.

[19] Liu Y, Duan Y, He Y, Yu C, Wang J, Huang J, Ye J, Parizel PM, Li K and Shu N. Whole brain white matter changes revealed by multiple diffusion metrics in multiple sclerosis: a TBSS study. Eur J Radiol 2012; 81: 2826-2832.

[20] Wang D, Qin W, Liu Y, Zhang Y, Jiang T and Yu C. Altered white matter integrity in the congenital and late blind people. Neural Plast 2013; 2013: 128236.

[21] Leming M, Steiner R and Styner M. A framework for incorporating DTI Atlas Builder registration into tract-based spatial statistics and a simulated comparison to standard TBSS. Proc SPIE Int Soc Opt Eng 2016; 9788: 97882S.
[22] Beaulieu C. The basis of anisotropic water diffusion in the nervous system - a technical review. NMR Biomed 2002; 15: 435-455.
[23] De Santis S, Drakesmith M, Bells S, Assaf Y and Jones DK. Why diffusion tensor MRI does well only some of the time: variance and covariance of white matter tissue microstructure attributes in the living human brain. Neuroimage 2014; 89: 35-44.
[24] Song SK, Sun SW, Ju WK, Lin SJ, Cross AH and Neufeld AH. Diffusion tensor imaging detects and differentiates axon and myelin degeneration in mouse optic nerve after retinal ischemia. Neuroimage 2003; 20: 1714-1722.
[25] Cao S, Song G, Zhang Y, Xie P, Tu Y, Li Y, Yu T and Yu B. Abnormal local brain activity beyond the pain matrix in postherpetic neuralgia patients: a resting-state functional MRI study. Pain Physician 2017; 20: E303-E314.
[26] Jiang J, Gu L, Bao D, Hong S, He W, Tan Y, Zeng X, Gong H, Zhang D and Zhou F. Altered homotopic connectivity in postherpetic neuralgia: a resting state fMRI study. J Pain Res 2016; 9: 877-886.
[27] Geha PY, Baliki MN, Wang X, Harden RN, Paice JA and Apkarian AV. Brain dynamics for perception of tactile allodynia (touch-induced pain) in postherpetic neuralgia. Pain 2008; 138: 641-656.
[28] Cole MW, Repovš G and Anticevic A. The frontoparietal control system: a central role in mental health. Neuroscientist 2014; 20: 652-664.
[29] Liu X, Gu L, Liu J, Hong S, Luo Q, Wu Y, Yang J and Jiang J. MRI study of cerebral cortical thickness in patients with herpes zoster and postherpetic neuralgia. J Pain Res 2022; 15: 623-632.
[30] Li W, Li Q, Zhu J, Qin Y, Zheng Y, Chang H, Zhang D, Wang H, Wang L, Wang Y and Wang W. White matter impairment in chronic heroin dependence: a quantitative DTI study. Brain Res 2013; 1531: 58-64.
[31] Squarcina L, Houenou J, Altamura AC, Soares J and Brambilla P. Association of increased genotypes risk for bipolar disorder with brain white matter integrity investigated with tract-based spatial statistics: special section on "Translational and Neuroscience Studies in Affective Disorders". Section Editor, Maria Nobile MD, PhD. This section of JAD focuses on the relevance of translational and neuroscience studies in providing a better understanding of the neural basis of affective disorders. The main aim is to briefly summarise relevant research findings in clinical neuroscience with particular regards to specific innovative topics in mood and anxiety disorders. J Affect Disord 2017; 221: 312-317.
[32] Mandl RC, Schnack HG, Zwiers MP, van der Schaaf A, Kahn RS and Hulshoff Pol HE. Functional diffusion tensor imaging: measuring task-related fractional anisotropy changes in the human brain along white matter tracts. PLoS One 2008; 3: e3631.
[33] Coppola G, Di Renzo A, Tinelli E, Petolicchio B, Di Lorenzo C, Parisi V, Serrao M, Calistri V, Tardioli S, Cartocci G, Caramia F, Di Piero V and Pierelli F. Patients with chronic migraine without history of medication overuse are characterized by a peculiar white matter fiber bundle profile. J Headache Pain 2020; 21: 92.
[34] Planchuelo-Gómez Á, García-Azorín D, Guerrero Á L, Aja-Fernández S, Rodríguez M and de Luis-García R. White matter changes in chronic and episodic migraine: a diffusion tensor imaging study. J Headache Pain 2020; 21: 1.
[35] Winklewski PJ, Sabisz A, Naumczyk P, Jodzio K, Szurowska E and Szarmach A. Understanding the physiopathology behind axial and radial diffusivity changes-what do we know? Front Neurol 2018; 9: 92.
[36] Lieberman G, Shpaner M, Watts R, Andrews T, Filippi CG, Davis M and Naylor MR. White matter involvement in chronic musculoskeletal pain. J Pain 2014; 15: 1110-1119.